STUDY ON UNDULATOR RADIATION FROM FEMTOSECOND ELECTRON BUNCHES

N. Chaisueb†, S. Rimjaem, Plasma and Beam Physics (PBP) Research Facility, Department of Physics and Materials Science, Faculty of Science, Chiang Mai University, Chiang Mai 50200, Thailand

Abstract

Linac-based terahertz (THz) source at the Plasma and Beam Physics (PBP) Research Facility, Chiang Mai University (CMU), Thailand, consists of a thermionic RF electron gun, an alpha magnet for magnetic bunch compressor, a travelling wave S-band accelerating structure for post acceleration, and various beam diagnostic instruments. The PBP-CMU linac system can produce relativistic femtosecond electron bunches, which are used to generate coherent THz radiation via transition radiation technique. To increase the radiation intensity, an electromagnetic undulator will be added in the beam transport line. The designed electromagnetic undulator has 35 periods with a period length of 64 mm and a pole gap of 15 mm. This study investigates the dependence of the electron beam energy and longitudinal bunch length on the coherent undulator radiation. The numerical simulation and procedure to generate the undulator radiation in the THz regime by using femtosecond electron bunches produced at the PBP research facility is reported and discussed in this contribution. Numerical calculation result shows that the energy of the undulator radiation, which is produced from electron bunches with an energy of 5 - 20 MeV, a peak current of 33 - 55 A, and an effective bunch length of 180 - 300 fs can reach 14 μJ.

INTRODUCTION

In the last decade, electromagnetic radiation in the THz regime has become interesting spectrum in many applications. The THz radiation can pass through non-metallic materials, but it is reflected by metal and is absorbed by liquid. Due to this unique characteristic, the THz radiation is used in several researches involved THz spectroscopy and non-destructive distinguish analysis of different density materials, e.g. THz imaging, which can be used in many applications. For examples, it is used to detect metallic and non-metallic weapons, explosive materials, and drugs through concealing obstacles such as clothing or packaging. Therefore, it is useful for airport security, homeland security and defense [1]. Moreover, it is possibly used to observe the correctness of the integrated circuits, such as semiconductor devices and electronic cards, which are enclosed in non-metallic package [2]. A tooth cavity in enamel and the cancerous region compared to the healthy region of human tissue can also be detected by THz imaging [3]. This leads to widely studies in development of THz light sources, detectors, and several experimental techniques.

†natthawut_chai@cmu.ac.th

At Chiang Mai University, relativistic electron bunches produced from the PBP-CMU linac system was firstly used to generate THz radiation by transition radiation technique in March 2006 [4]. The electron beam is produced from the RF-gun with the maximum kinetic energy of about 2 - 2.5 MeV and a bunch length of around 100 - 200 ps [5]. The beam with long bunch length was then compressed and accelerated by using the alpha magnet and the travelling wave s-band linac structure, respectively. Then, it arrives at the experimental station with the bunch length of 180 - 300 fs and the total energy of 10 - 15 MeV. Transition radiation is emitted when electrons passing through a boundary between two different dielectric media. At the PBP facility, a thin Al-foil was placed in the electron's path at the experimental station. Then, the radiation is emitted from the interface between vacuum and the Al-foil resulting from an electric field discontinuity at the transition area of the materials with different dielectric constants. The radiation was, then, measured by using a Michelson interferometer and a pyroelectric detector. The spectrum of the THz transition radiation generated from electron beam with an electron energy of 10 MeV and a bunch length of 200 fs overs the wave number of about 80 cm^{-1} with the radiation energy of around 9 - 22 μJ per macropulse [4]. The produced THz radiation was used to create THz images via a transmission mode of imaging technique for several materials, such as cut-pattern in Al-foils, raw and cooked rice grains, water drop, and a fresh leaf [4].

The power of the THz radiation generated from the present setup of the PBP-CMU linac via transition radiation is merely in milliwatt scale resulting in low-resolution THz images. Therefore, a plan to increase the power or the intensity of the THz radiation by using a coherent undulator radiation method is conducted. This is in order to be able to apply the THz radiation in various researches for distinguishing material components with high resolution.

UNDULATOR MAGNET

In the future setup of the accelerator system, an electromagnetic undulator will be inserted as the new experimental station in the beam line as shown in Fig. 1. Typical undulator magnets compose of a periodic structure of dipole magnets. A static magnetic field is alternating along the length of the undulator with a certain period length. Electrons in a short bunch moving through the undulator magnetic field are oscillating in the transverse direction and emitting the radiation coherently. Therefore, the undulator radiation of femtosecond

ISBN 978-3-95450-134-2

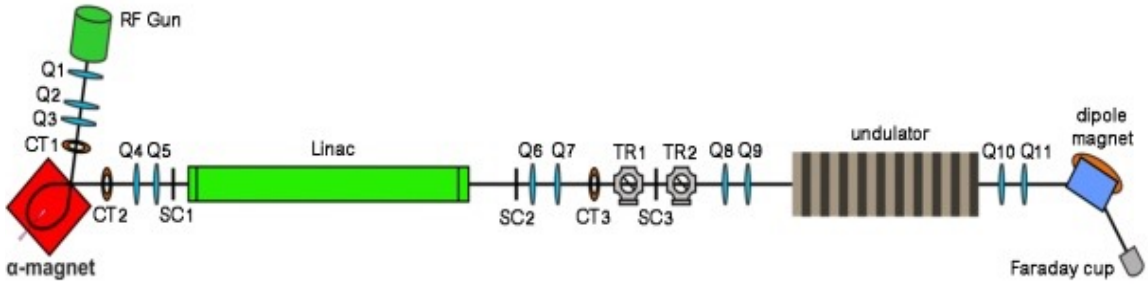

Figure 1: Future setup of the PBP CMU-linac with undulator magnet. The letters Q, CT, SC and TR represent quadrupole magnets, current transformers, screen stations, and transition radiation stations.

electron bunches is very intense, coherence, and is concentrated in the narrow band of spectrum.

An undulator radiation wavelength (λ_r) depends on undulator period length (λ_u), undulator parameter (K), and electron beam energy (E) as [6]

$$\lambda_r = \frac{\lambda_u}{2n\gamma^2}\left(1+\frac{K^2}{2}+\theta^2\gamma^2\right), \quad (1)$$

where $\gamma = E/m_e c^2$ is the Lorentz factor, m_e is the rest mass of electron and c is the speed of light. The harmonic number (n) is integer numbers 1,2,3,… and θ is the angle of observation related to the average beam direction. The undulator parameter can be calculated by using the following equation [6]

$$K = \frac{eB_0\lambda_u}{2\pi m_e c} = 0.934 B_0 \lambda_u, \quad (2)$$

where B_0 is the peak magnetic field of the undulator. For $K \ll 1$, the fundamental harmonic ($n = 1$) is only considered. For $K \geq 1$, the radiation power is maximum at the fundamental harmonic and it is more intense for the first few harmonics.

The undulator magnet is designed and simulated for both 2D and 3D models with the computer codes SUPERFISH [7] and RADIA [8], correspondingly. Preliminary, this electromagnetic undulator consists of 71 magnet poles, return yokes and conducting coils. The pole number was correctly defined to be an odd number in order to have enough number of poles to guide the electron trajectory back to the mid-plane of the magnet. The number of period (N_p) is 35 periods with a period length of 64 mm and the pole gap of 15 mm. The maximum period number is limited by the length of available space for installation of the undulator magnet, which will be located downstream the linac and the transition radiation stations (TR1 and TR2) as shown in Fig. 1. This available space is around 2 - 2.5 m.

The undulator parameter or the magnetic field strength of the undulator can be adjusted by varying the coils' current or the width of the pole gap. Due to limitation of a vacuum chamber height located in the gap of the undulator, the desired undulator parameter will be reached by adjusting the coils' current. The magnetic field of the undulator is alternating in the vertical direction throughout the magnet length. Consequently, the field on the undulator axis of each pair of magnet poles (upper and lower poles) is similar to that of a dipole magnet, which is given by [9]

$$B_0 = \frac{\mu_0 NI}{h}, \quad (3)$$

where NI is the total coils current in terms of number of turns in a conducting coil and the current, h is the magnet pole gap, and μ_0 is the permeability in the vacuum. The relation between the undulator parameter and the total current considered from equation (2) and (3) is shown in Fig. 2. It shows that the undulator parameter obviously has a linear relation with the total current.

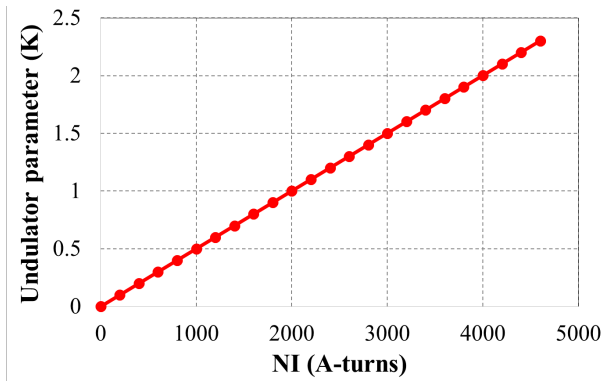

Figure 2: The undulator parameter as a function of the total current of the conducting coils.

Currently, the PBP-CMU linac system can produce femtosecond electron bunches with a typical electron energy up to 15 MeV. Higher beam energies (~20 - 25 MeV) can be achieved with higher feeding RF power. To study the dependence of the undulator specifications on the electron beam energy, we consider 5 cases of 5, 7, 10, 15, and 20 MeV electron beams. Then, the undulator wavelength and the undulator parameter are determined by using equations (1) and (2) for the first harmonic ($n = 1$) and only for on-axis radiation ($\theta = 0$). The calculated

ISBN 978-3-95450-134-2

wavelength as a function of the undulator parameter for various electron beam energies is shown in Fig. 3.

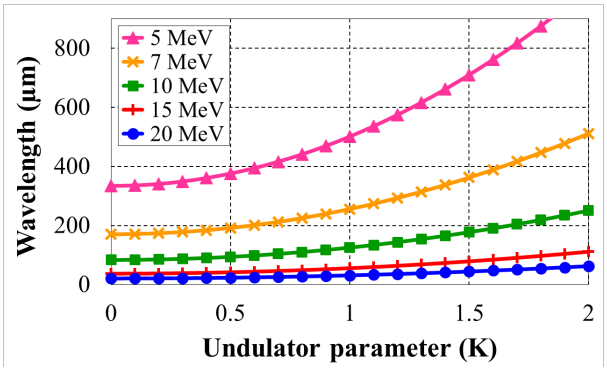

Figure 3: The undulator radiation wavelength as a function of the undulator parameter for the electron energies of 5, 7, 10, 15 and 20 MeV.

The undulator parameter is considered to be around 1, which is not required too high magnetic field. Figure 3 indicates that the wavelength range of the output radiation gets broader as the electron energy decreases for the undulator parameter up to 1. The wavelength of around 30 - 500 μm can be obtained at the undulator parameter of 1 with the total current of 2000 A-turns for electron beam energies of 10 MeV.

UNDULATOR RADIATION

The undulator radiation emitted from relativistic electrons subjected into periodic fields will be considered as the coherent synchrotron radiation (CSR) when the electron bunch length is equal or shorter than the radiation wavelength. This leads to properly add up of the emitted radiation from individual undulator poles in the forward direction and results in the enhancement of the radiation brightness as the brightness of the coherent radiation is proportional to the electron number squared. The defecting angle of the electron beam traveled in the undulator is no larger than the natural opening angle of the emission pattern in the laboratory frame. Consequently, the emitted radiation is collimated in forward direction and has narrow spectral range at a well-specified wavelength [10]. Nevertheless, the required spectral regime of the undulator radiation can be shifted by changing the undulator parameter that can be varied via adjusting the current of the conducting coils of the undulator magnet.

The total CSR energy (W_{coh}) depends on the radiation energy of a single electron (W_{1e}), the number of electron (N_e) squared, and the form factor (f_k) squared given by [11]

$$W_{coh} = W_{1e} N_e^2 f_k^2, \tag{4}$$

where

$$W_{1e} = \frac{\pi q_e^2 N_p}{3\varepsilon_0 \lambda_u} K^2 \gamma^2. \tag{5}$$

Here, q_e is the electron charge and ε_0 is the permittivity of free space. Typically, the form factor of the electron beam with the bunch length (σ) can be estimated to be the Gaussian distribution with a standard deviation (σ), where k is the wave vector expressed by [11]

$$f_k = e^{-\sigma^2 k^2}. \tag{6}$$

The emanated radiation features depend on the specific properties of the electron beam and the undulator magnet. The electron bunch charge (Q) at the experimental station is considered to be 25 pC which is equal to electrons [4]. This value was regarded throughout the calculation in this section. The peak current ($\hat{I}$) is defined by the bunch charge and the bunch length to be about 33 - 55 A, which can be calculated by the well-known formula

$$\hat{I} = \frac{Q}{\tau_{eff}} = \frac{Q}{\sqrt{2\pi}\sigma}, \tag{7}$$

where τ_{eff} is the effective bunch length. Specifications of the electron beam produced from the PBP-CMU linac and the designed undulator magnet are shown in Table 1.

Table 1: Summary of Electron Beam Properties of PBP-CMU Linac and The Designed Undulator Magnet

Parameters	Value
Electron beam at the undulator entrance	
Electron energy	5 - 20 MeV
Bunch charge	25 pC
Bunch length	180 - 300 fs
Peak current	33 - 55 A
Designed undulator magnet	
Undulator parameter	≈1
Period length	64 mm
Number of periods	35 periods
Pole gap	15 mm

The CSR wavelength as a function of the form factor for the electron bunch length of 180, 240, and 300 fs are presented in Fig. 4. The form factor is smaller when the electron bunch length increases or the electron bunch expands longitudinally. The calculation results in Fig. 4 show the proportional relation between the CSR wavelength and the form factor of electron beam. The radiation wavelength range generated from the short electron bunch is broader than that of the long electron bunch when considering in the form factor of 0.001 - 1.

ISBN 978-3-95450-134-2

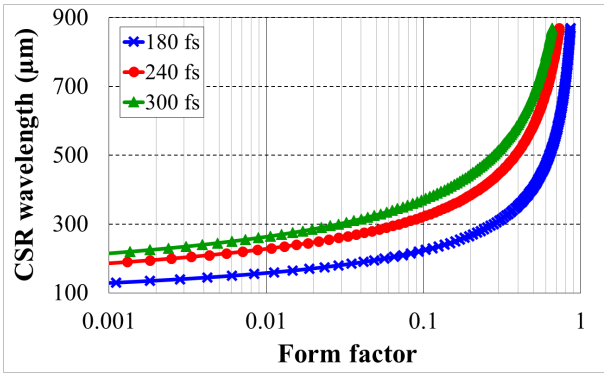

Figure 4: The CSR wavelength versus the electron form factor for the electron bunch length of 180, 240, and 300 fs.

Furthermore, Fig. 5 also shows the relation between the total CSR energy and the CSR wavelength considered for the chosen electron energy of 10 MeV and the bunch length of 180, 240, and 300 fs.

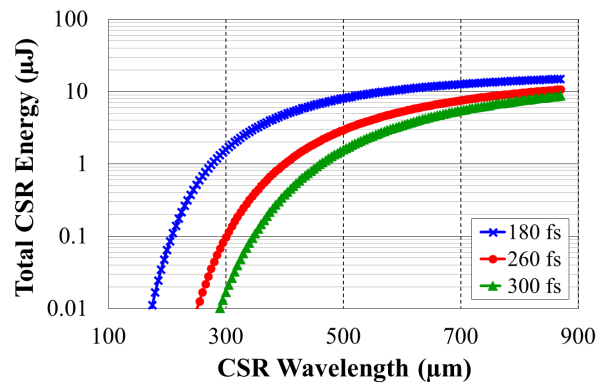

Figure 5: The total CSR energy as a function of the CSR wavelength for the electron bunch length of 180, 240 and 300 fs.

The graphs in Fig. 5 indicates that the total CSR energy is logarithmically increases and then saturates up to about 10 μJ at the CSR wavelength of 800 μm for all three bunch lengths. The radiation energy is higher when the electron bunch length is shorter at certain wavelength. When the 10 MeV electron beam with a bunch length of 180 fs and a bunch charge of 25 pC travels in the magnetic field of the undulator magnet with the undulator parameter of 1 and the undulator gap of 15 mm, the CSR energy of up to 14 μJ per microbunch can be obtained.

In general, the spectral brightness is determined to be the number of photons per second per unit solid angle per unit solid area in a constant fractional bandwidth [10]. While the width of the peak is a function of the number of undulator periods, the transverse size, and the divergence of the electron beam [12]. Preliminary study of the spectrum is considered by using the radiation simulation program called B2E with the ideal sinusoidal magnetic field. The ideal angular flux density, which is often used instead to present the radiation brightness, is calculated from the 10 MeV electron beam and the peak undulator field of 0.1674 T ($K \approx 1$) for the bunch lengths of 180, 240, and 300 fs. The results are shown in Fig. 6.

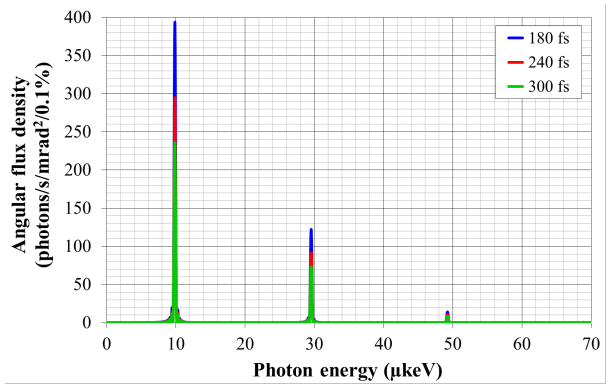

Figure 6: Angular flux density as a function of photon energy with the electron energy of 10 MeV for the bunch lengths of 180, 240, and 300 fs.

The result shows that the angular flux density at the fundamental harmonic for all electron bunch lengths is accomplished at the photon energy of 9.85 μkeV with a quasi-monochromatic peak of spectrum. Moreover, the angular flux density increases when the bunch length is shorter.

CONCLUSION

Preliminary study on coherent undulator radiation from femtosecond electron bunches was conducted. The undulator radiation wavelength and energy are tunable by adjusting the current of the conducting coils of the undulator magnet. The calculation results show that the radiation wavelength of around 30 - 500 μm can be obtained for the electron beam energies of 5 - 20 MeV. When the shorter electron bunch length is achieved, the short radiation wavelength is generated with the high radiation energy and high brightness. Further study with actual undulator magnetic field will be continue to study the performance of the setup.

ACKNOWLEDGEMENTS

The authors would like to express our essential gratitude to K. Thaijai-un for his initial design of the undulator. We would like to acknowledge the support by the Department of Physics and Materials Science, Faculty of Science, Chiang Mai University and the Science Achievement Scholarship of Thailand.

REFERENCES

[1] Wai Lam Chan et al., Rep. Prog. Phys. 70, 1325 (2007).
[2] G. P. Gallerano et al., J. Infrared. Milli. Terhz Waves 30, 1351 (2009).
[3] P. C. Ashworth et al., Opt. Express 17, 12444 (2009).

ISBN 978-3-95450-134-2

[4] J. Saisut, Ph.D Thesis, Chiang Mai University, (2011).
[5] S. Rimjaem et.al., Nucl. Instr. Meth. Phys. Res., Sect. A 10, 736 (2014).
[6] J. A. Clarke, *The Science and Technology of Undulators and Wigglers*, (New York: OUP, 2004), 231.
[7] L. M. Young, J. H. Billen, POISSON/SUPERFISH, Technical Note No. LA-UR-96-1834, Los Alamos National Laboratory (2006).
[8] RADIA, http://www.esrf.eu/Accelerators/Groups/InsertionDevices/Software/Radia
[9] K. Wille, *The Physics of Particle Accelerators*, (New York: OUP, 2000), 315.
[10] G. Brown et.al., Nucl. Instr. Meth. Phys. Res. 65, 208 (1983).
[11] D. Bocek, Ph.D Thesis, Stanford University, (2006).
[12] H. Winick et.al., Phys. Today 50, 34 (1981).

ISBN 978-3-95450-134-2